Available online at www.sciencedirect.com
ScienceDirect
International Journal of Pharmaceutics 351 (2008) 259–270
INTERNATIONAL JOURNAL OF PHARMACEUTICS
www.elsevier.com/locate/ijpharm

Pharmaceutical Nanotechnology

Enhanced antitumor activity of combinations of free and HPMA copolymer-bound drugs

J. Hongrapipat [a,b], P. Kopečková [a], S. Prakongpan [b], J. Kopeček [a,c,*]

[a] *Department of Pharmaceutics and Pharmaceutical Chemistry, University of Utah, Salt Lake City, UT 84112, USA*
[b] *Department of Pharmacy, Mahidol University, Bangkok 10400, Thailand*
[c] *Department of Bioengineering, University of Utah, USA*

Received 28 June 2007; received in revised form 25 August 2007; accepted 17 September 2007
Available online 22 September 2007

Abstract

The synergism in anticancer effect toward human renal carcinoma A498 cells by binary combinations of free and *N*-(2-hydroxypropyl)methacrylamide (HPMA) copolymer-bound anticancer drugs, SOS thiophene (SOS), doxorubicin (DOX), and mesochlorin e_6 monoethylenediamine (Mce_6), was evaluated. The combination index (CI) analysis was used to quantify the synergism, antagonism, and additive effects. Both free drugs and HPMA copolymer conjugates, when used as single agents or in combination, exhibited cytotoxic activities against A498 cells, as determined using a modified MTT assay. As single agents, SOS and P-GFLG-SOS (HPMA copolymer conjugates containing SOS bound via glycylphenylalanylleucylglycine [GFLG] spacer) were significantly more effective than the other agents evaluated. The synergistic effects ranked in the order SOS + DOX > P-GFLG-DOX + P-GFLG-Mce_6 ≈ DOX + Mce_6 > P-GFLG-SOS + P-GFLG-DOX ≈ SOS + Mce_6 > P-GFLG-SOS + P-GFLG-Mce_6. The combination of SOS + DOX proved to be synergistic over all cell growth inhibition levels. All other combinations exhibited synergism in a wide range of drug effect levels. The SOS + Mce_6 and P-GFLG-SOS + P-GFLG-Mce_6 combinations displayed synergism up to drug affected fraction (f_a) values of about 0.8 and reached slight antagonism and nearly additivity at $f_a = 0.95$, respectively. However, all other combinations were synergistic up to $f_a < 0.9$ and were additive at higher f_a values. The observations that most combinations produced synergistic effects will be important for clinical translation.

Keywords: *N*-(2-Hydroxypropyl)methacrylamide (HPMA) copolymer; 2,5-*bis*(6-hydroxymethyl-2-thienyl)furan; Doxorubicin; Mesochlorin e_6 monoethylenediamine; Combination index; Renal cancer

1. Introduction

Renal cell carcinoma accounts for about 3% of adult malignancies and is by far the most frequent neoplasm arising from the kidney. The prognosis for advanced stage renal carcinoma is poor. The low efficiency of chemotherapeutic agents is due to high levels of *p*-glycoprotein expression in normal renal proximal tubules and renal carcinoma cells (Mickisch et al., 1990; Kim et al., 1996). Moreover, about one-third of patients develop metastatic disease after nephrectomy (Sachdeva, 2006). Evidently, novel approaches in the treatment of renal carcinoma are needed.

It is well known that macromolecular drug delivery systems have the potential to overcome multidrug resistance. The exclusion of the polymer–drug conjugates from the cytoplasm of the cell, due to the fact that intracellular trafficking occurs within membrane-limited organelles, renders efflux pumps ineffective (Kopeček et al., 2000). Experimental data on sensitive (A2780) and resistant (A2780/AD) human ovarian carcinoma cells showed that, in contrast to free doxorubicin (DOX), *N*-(2-hydroxypropyl)methacrylamide (HPMA) copolymer-bound DOX (P-GFLG-DOX, where P is the HPMA copolymer backbone) overcame pre-existing MDR1-gene-encoded multidrug resistance, and did not induce it *de novo* after acute or chronic exposure *in vitro* (Minko et al., 1998, 1999). Similar results were obtained in solid tumor mice models of DOX sensitive

* Corresponding author at: Department of Pharmaceutics and Pharmaceutical Chemistry, University of Utah, 30 S. 2000 E. Rm. 201, Salt Lake City, UT 84112, USA. Tel.: +1 801 581 7211; fax: +1 801 581 7848.
E-mail address: jindrich.kopecek@utah.edu (J. Kopeček).

0378-5173/$ – see front matter © 2007 Elsevier B.V. All rights reserved.
doi:10.1016/j.ijpharm.2007.09.018

and resistant human ovarian carcinoma. Free DOX was effective only in sensitive tumors, while P-GFLG-DOX was effective in both sensitive and drug-resistant tumors (Minko et al., 2000).

To improve the therapeutic outcome and reduce the toxicity of anticancer agents, combination treatments have been developed and studied (Frei et al., 1965). For example, combinations of chemotherapies using agents with different mechanisms of action (Harris et al., 2005; Shanks et al., 2005); chemotherapy in combination with photodynamic therapy (PDT) (Nahabedian et al., 1988; Jin et al., 1992; Peterson et al., 1995); chemotherapy and immunotherapy (Welt et al., 2003); PDT and radiotherapy (Colasanti et al., 2004); and radioimmunotherapy with radiotherapy (Buchegger et al., 2000) have been studied.

Recently, a novel concept of using combination therapy with water-soluble polymer bound drugs was developed (Kopeček and Krinick, 1993). *In vivo* combination chemotherapy and PDT studies on two cancer models, Neuro 2A neuroblastoma induced in A/J mice (Krinick et al., 1994) and human ovarian carcinoma heterotransplanted in nude mice (Peterson et al., 1996; Shiah et al., 2000, 2001b), demonstrated that combination therapy with HPMA copolymer-bound DOX and HPMA copolymer-bound Mce_6 (mesochlorin e_6 monoethylenediamine) produced tumor cures which could not be obtained with either chemotherapy or PDT alone. Additionally, significantly lower non-specific toxicities were observed when compared to low-molecular weight drugs.

The most commonly used method to evaluate drug combinations *in vitro* is median-effect analysis, based on the Loewe additivity model, as originally proposed by Chou and Talalay (Chou and Talalay, 1984; Zhao et al., 2004; Chou, 2006). The median-effect method assesses the drug–drug interaction by a term called the "combination index" (CI), which is based on the concentration–response relationship. Numerous anticancer agent combinations had been analyzed using the median-effect method. Examples include: combination therapy for chronic myelogenous leukemia with imatinib and γ-irradiation or alkylating agents (busulfan and treosulfan) (Topaly et al., 2002); the combination treatment of lung adenocarcinoma cell line using perifosine and 7-hydroxystaurosporine (Dasmahapatra et al., 2004); and combination treatment using irofulven and 5-fluorouracil or cisplatin against human colon and ovarian carcinoma cells (Poindessous et al., 2003).

The novel anticancer agent 2,5-*bis*(6-hydroxymethyl-2-thienyl)furan (SOS, NSC 652287) is a dithiophene compound possessing a potent and selective activity against human renal cancer cell lines. The mechanism of action of SOS has been shown to block the p53–HDM-2 (human double minute-2) interaction *in vitro* and *in vivo* in various tumor cells lines expressing wild-type p53, such as the A498 cell line. In SOS treated cells, p53 levels increase, inducing cell cycle arrest and apoptosis (Nieves-Neira et al., 1999; Rivera et al., 1999; Fischer and Lane, 2004; Issaeva et al., 2004).

The anthracycline antitumor antibiotic DOX is one of the most effective chemotherapeutic agents. DOX inhibits the activity of topoisomerase II, produces non-protein-associated DNA strand breaks, and generates free radicals, creating DNA damage within the cells, cellular membrane damage, and ultimately cell death (Fornari et al., 1994).

Mce_6 is the second-generation synthetic photosensitizer. When activated by light, it interacts with molecular oxygen to produce highly reactive singlet oxygen, causing irreversible photodamage to cells resulting in cell death (Hopper, 2000).

In this study, SOS, DOX, and Mce_6 were chosen as anticancer agents; these represent low-molecular weight compounds possessing different sites and/or mechanisms of action. The interactions between free and HPMA copolymer-bound SOS, DOX, and Mce_6 in binary combination against the A498 renal carcinoma cell line *in vitro* were evaluated using median-effect analysis. We hypothesized that a combination of these agents may produce synergistic effects and thereby reduce effective doses, compared to the doses required for each agent alone to produce a given drug effect level.

2. Materials and methods

2.1. Abbreviations

CI, combination index; D_m, median-effect dose; DI, deionized; DIPEA, *N*,*N*-diisopropylethylamine; DMAP, 4-dimethylaminopyridine; DMF, *N*,*N*-dimethylformamide; DMSO, dimethylsulfoxide; DOX, doxorubicin hydrochloride; DRI, dose-reduction index; EPR, enhanced permeability and retention; GFLG, glycylphenylalanylleucylglycine; HPMA, *N*-(2-hydroxypropyl)methacrylamide; IC_{50}, concentration that inhibited cell growth by 50% as compared with control cell growth; MA, methacryloyl; M_n, number average molecular weight; M_w, weight average molecular weight; Mce_6, mesochlorin e_6 monoethylenediamine disodium salt; MRP, multidrug resistance-related protein; MTT assay, modified 3-(4,5-dimethylthiazol-2-yl)-2,5-diphenyltetrazoliumbromide assay; ONp, *p*-nitrophenoxy; P, HPMA copolymer backbone; PDT, photodynamic therapy; P-GFLG-DOX, HPMA copolymer–DOX conjugate; P-GFLG-Mce_6, HPMA copolymer–Mce_6 conjugate; P-GFLG-ONp, HPMA copolymer precursor containing reactive *p*-nitrophenyl ester groups at side chain termini; P-GFLG-SOS, HPMA copolymer–SOS conjugate; SOS, 2,5-*bis*(5-hydroxymethyl-2-thienyl)furan.

2.2. Materials

SOS was kindly supplied by the National Cancer Institute. DOX was a gift from Dr. A. Suarato, Pfizer, Milano, Italy. Mce_6 was purchased from Porphyrin Products (Logan, UT). All other chemicals were purchased from Sigma Chemical Co. (St. Louis, MO).

2.3. Cell lines

The human renal carcinoma cell line A498 was purchased from American Type Culture Collection (ATCC). Cells were grown as monolayer cultures in EMEM medium (ATCC, Manassas, VA) supplemented with 10% fetal bovine serum (HyClone

Laboratories, Logan, UT), at 37 °C in a humidified atmosphere of 5% CO_2 (v/v).

2.4. Synthesis of HPMA copolymer–drug conjugates

2.4.1. HPMA copolymer–SOS conjugate (P-GFLG-SOS)

P-GFLG-SOS was synthesized using a polymer analogous reaction in two steps. First, the polymer precursor (P-GFLG-ONp) was prepared by radical precipitation copolymerization of HPMA and *N*-methacryloyl glycylphenylalanylleucylglycine *p*-nitrophenyl ester (MA-GFLG-ONp; Kopeček et al., 1991; Ulbrich et al., 2000). The polymer precursor contained 4.15 mol% of active ester groups; molecular weight (M_w) = 23 kDa; polydispersity (M_w/M_n) = 1.3. Second, SOS was bound to P-GFLG-ONp by an ester linkage. The reactions are shown in Scheme 1. P-GFLG-ONp (450 mg, 0.116 mmol ONp groups) was dissolved in *N*,*N*-dimethylformamide (DMF; ~4 ml). SOS (71 mg, 0.243 mmol) was dissolved in DMF (~1 ml). Polymer precursor solution was then mixed with the SOS solution. 4-Dimethylaminopyridine (DMAP; 40 mg, 0.327 mmol) was added into the reaction mixture. The reaction solution was bubbled with N_2 and allowed to proceed for 72 h in the dark at room temperature. The DMF was then partially evaporated to ~2 ml under reduced pressure. The product was precipitated in a mixture of acetone:ether (3:1 (v/v), ~550 ml). The precipitate was collected by filtration, washed with acetone (~50 ml) and ether (~50 ml), and dried under vacuum. To purify the product was dissolved in methanol (~3 ml) and applied to a Sephadex LH-20 column with methanol as the mobile phase. The polymer band was collected, concentrated under reduced pressure and re-precipitated. The product was a yellowish powder, with a yield of 340 mg (61%). The characterization of the polymer conjugates is shown in Table 1.

2.4.2. HPMA copolymer–DOX conjugate (P-GFLG-DOX)

P-GFLG-DOX was prepared as described previously (Kopeček et al., 1991; Krinick et al., 1994). Briefly, the conjugate

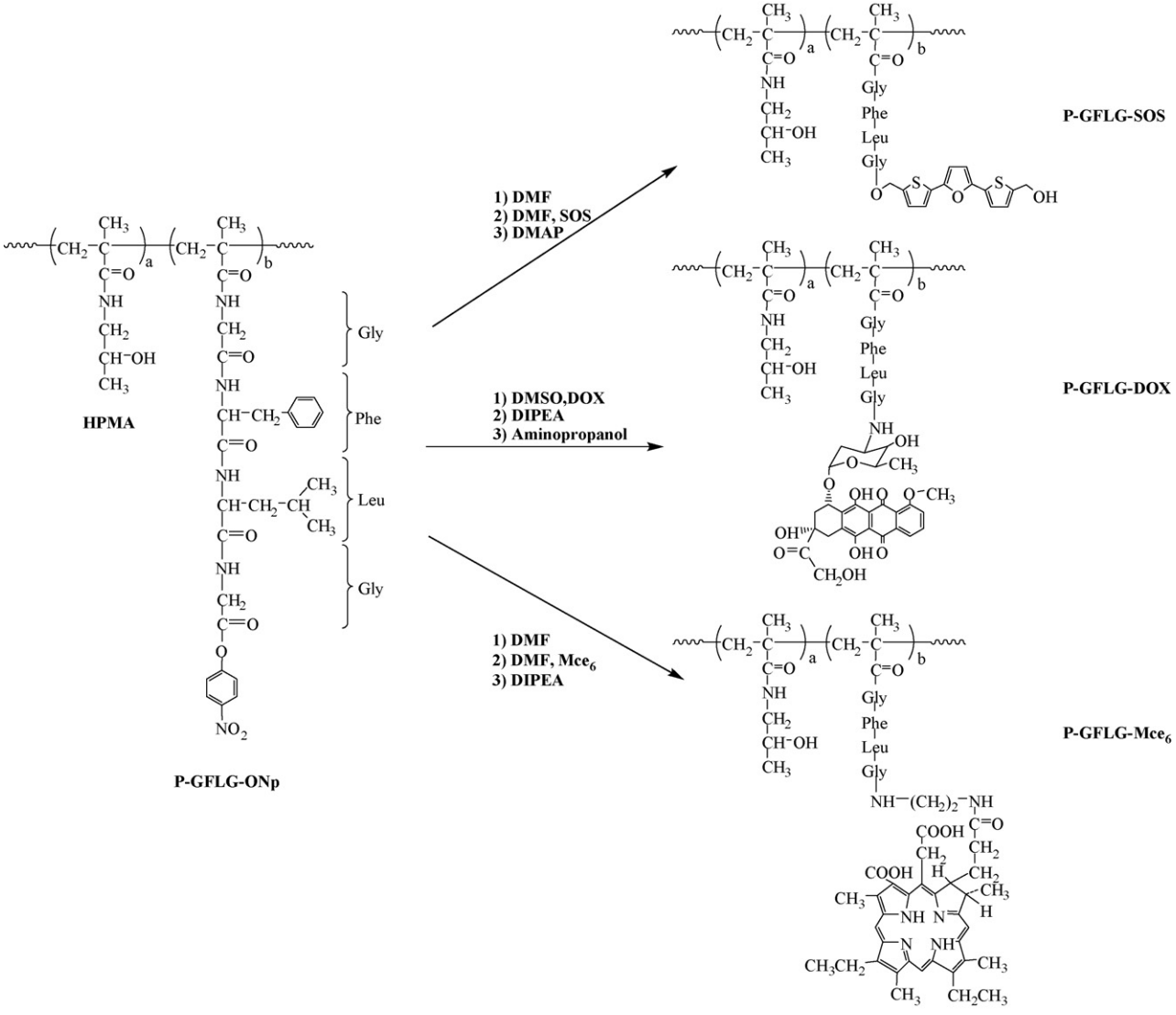

Scheme 1. Synthesis and chemical structure of *N*-(2-hydroxypropyl)methacrylamide (HPMA) copolymer–SOS/–DOX/–Mce_6 conjugates (P-GFLG-SOS, P-GFLG-DOX, and P-GFLG-Mce_6, respectively) containing glycylphenylalanylleucylglycine spacers.

Table 1
Characterization of HPMA copolymer–drug conjugates

Conjugates	Mol% of drug[a]	mmol drug per g polymer conjugate	Number of drug molecules per macromolecule	Apparent M_w (kDa)[b]	Polydispersity[c]
P-GFLG-SOS	1.62	0.106	3.4 (SOS)	32	1.50
P-GFLG-DOX	1.93	0.121	3.0 (DOX)	25	1.24
P-GFLG-Mce_6	2.04	0.125	2.9 (Mce_6)	23	1.34

[a] Determined by UV spectrophotometry (extinction coefficient at 358 nm (ε_{358}) = 33,000 M^{-1} cm^{-1} in methanol for SOS, ε_{488} = 11,000 M^{-1} cm^{-1} in DI water for DOX, and ε_{395} = 158,000 M^{-1} cm^{-1} in methanol for Mce_6).

[b] Apparent molecular weight (M_w) of polymers was estimated by size exclusion chromatography using a fast performance liquid chromatography (FPLC) system equipped with a Superose 6 column, calibrated with polyHPMA fractions. Acetate buffer pH 5.5 + 30% (v) acetonitrile was used for P-GFLG-SOS. PBS buffer pH 7.3 + 30% (v) acetonitrile was used for P-GFLG-DOX and P-GFLG-Mce_6.

[c] Polydispersity = the ratio of weight-average to number-average molecular weight.

was synthesized by conjugating DOX to P-GFLG-ONp precursor, containing 5.5 mol% of active ester groups; M_w = 22 kDa; M_w/M_n = 1.2. The procedure is shown in Scheme 1. DOX (127 mg, 0.220 mmol) and P-GFLG-ONp (1 g, 0.330 mmol ONp groups) were dissolved in dimethylsulfoxide (DMSO; ~4 ml). The reaction mixture was stirred to complete dissolution for 20 min. *N*,*N*-Diisopropylethylamine (DIPEA; 48 μl, 0.275 mmol) was added while stirring. The reaction mixture was stirred overnight in the dark at room temperature. Then, 1-amino-2-propanol (~15 μl) was added under stirring. The reaction mixture was precipitated into a mixture of acetone:ether (3:1 (v/v), ~500 ml). The precipitate was collected by filtration, washed with a mixture of acetone:ether (3:1, (v/v)) and ether, and dried under vacuum. The product was dissolved in methanol (~10 ml) and purified twice on a Sephadex LH-20 column with methanol/0.5% acetic acid as the mobile phase. The polymer band was then collected and evaporated to dryness. The product was dissolved in deionized (DI) water (~20 ml), dialyzed overnight against DI water and lyophilized. The product yield was 820 mg (68%).

2.4.3. HPMA copolymer–Mce_6 conjugate (P-GFLG-Mce_6)

P-GFLG-Mce_6 was also prepared as described previously (Kopeček et al., 1991; Krinick et al., 1994). The conjugate was synthesized by conjugating Mce_6 to P-GFLG-ONp precursor, containing 5.1 mol% of active ester groups; M_w = 22 kDa; M_w/M_n = 1.2. The procedure is shown in Scheme 1. Mce_6 (160 mg, 0.234 mmol) was dissolved in DMF (~3 ml). P-GFLG-ONp (750 mg, 0.230 mmol ONp groups) was dissolved in DMF (~2.5 ml). The suspension of Mce_6 was added dropwise into polymer precursor solution while stirring. The reaction mixture was stirred for 1 h until the mixture was completely dissolved. DIPEA (40 μl, 0.229 mmol) was added under stirring. The solution was stirred overnight in the dark at room temperature. The solution was precipitated into a mixture of acetone:ether (3:2 (v/v), ~500 ml). The precipitate was collected by filtration and dried under vacuum. The product was dissolved in methanol (~10 ml) and purified twice on a Sephadex LH-20 column with methanol/0.5% acetic acid as the elution solvent. The polymer band was collected and evaporated to dryness. The product was dissolved in DI water (~20 ml), dialyzed overnight and lyophilized. The product yield was 670 mg (69%).

2.5. Drug stock solution preparations

SOS was dissolved in PBS containing cyclodextrin (5% (w/v) cyclodextrin in PBS/1 mg of SOS) to enhance the solubility of SOS (Alley et al., 2004). Other samples (DOX, Mce_6, P-GFLG-SOS, P-GFLG-DOX, and P-GFLG-Mce_6) were prepared in DI water. All stock solutions were filtered using 0.22 μm sterile filter and kept in sterilized Eppendorf tubes. Drug contents were determined by UV spectrophotometry. All stock solutions were freshly prepared and gradually diluted with EMEM culture medium before use.

2.6. In vitro growth inhibition bioassays

The drug concentration that inhibited cell growth by 50% compared with control cells (IC_{50}) was determined using a modified 3-(4,5-dimethylthiazol-2-yl)-2,5-diphenyltetrazoliumbromide (MTT) assay (Hansen et al., 1989). Cells were seeded in 96-well flat bottom microplates at a density of 5000 cells/well in 200 μl of EMEM medium and allowed to grow for 36 h. The cells were then exposed to various concentrations of each free drug alone (SOS, DOX, and Mce_6), each copolymer conjugate (P-GFLG-SOS, P-GFLG-DOX, and P-GFLG-Mce_6), or their binary combinations (n = 6). After 16 h of exposure, the drugs were removed, cells were washed with warm PBS and the medium (300 μl) replaced. For the cell growth inhibition studies using Mce_6 or P-GFLG-Mce_6 (alone or in combinations), the cells were irradiated with three tungsten halogen lamps through a 650 nm band pass filter at 3.0 mW/cm^2 for 30 min. After an additional 3 days in culture, medium was removed and replaced with 100 μl of fresh medium and 10 μl of sterile-filtered MTT solution (5 mg/ml in PBS). After incubating for 24 h, 150 μl of 20% (w/v) sodium dodecyl sulfate in water was added to each well and incubated overnight. The following day, the absorbance of each well was read at 570 nm with a reference wavelength at 630 nm. Untreated cells served as a

100% cell viability control and the media served as background reference. Growth inhibition was expressed as the growth of drug-treated cells related to that of untreated control cells.

2.7. Dose–effect analysis and determination of combination index (CI)

In binary combination treatment studies, A498 cells were treated with a dose range of SOS, DOX, Mce_6, P-GFLG-SOS, P-GFLG-DOX, and P-GFLG-Mce_6 simultaneously ($n = 6$). Drug interactions and CI values were analyzed using median-effect principle according to the method of Chou and Talalay (Chou and Talalay, 1984; Chou, 2006).

The median-effect equation describes dose–effect relationships, which is described by

$$\frac{f_a}{f_u} = \left(\frac{D}{D_m}\right)^m \quad (1)$$

where f_a and f_u are the fraction affected [1 − (absorbance of treatment well − average of absorbance of blanks)/(average of absorbance of untreated cell wells − average of absorbance of blanks)] and unaffected ($f_u = 1 - f_a$) by the dose or concentration D, D_m is the median-effect dose (IC_{50}) that inhibits the cell growth by 50%, and m is the coefficient signifying the shape of the dose–effect relationship.

Based on the logarithmic conversion of Eq. (1) (Chou, 1976):

$$\log\left(\frac{f_a}{f_u}\right) = m\log(D) - m\log(D_m) \quad (2)$$

where m is the slope and D_m is the anti-log of the x-intercept. The plot of $x = \log(D)$ versus $y = \log(f_a/f_u)$ is called the median-effect plot. An example is shown in Fig. 1 for the SOS + DOX combination, including the dose–effect curves and the median-effect plots.

The combination index (CI) describes the interaction between two drugs and quantitates the synergism, antagonism or additive effects. The CI is determined by the equation:

$$CI = \frac{(D)_1}{(D_x)_1} + \frac{(D)_2}{(D_x)_2} \quad (3)$$

where $(D_x)_1$ and $(D_x)_2$ are the doses of drug 1 alone and drug 2 alone that inhibit the cell growth x%, respectively. $(D)_1$ and $(D)_2$ are for doses in combination that also inhibit x%.

The CI values were calculated by solving Eq. (3) for different values of f_a and plotting the CI values as a function of f_a values, using CompuSyn software (ComboSyn Inc., Paramus, NJ). In the f_a–CI plot, CI < 1, =1, and >1 indicate synergism, additivity, and antagonism, respectively.

The dose-reduction index (DRI) (Chou and Martin, 2006) is a determination of how many times the dose of each drug in a synergistic combination may be reduced at a given effect level compared with the doses of each drug alone. The dose reduction is an indication of how toxicity is reduced toward normal cells or host while the desired therapeutic effect is maintained. The

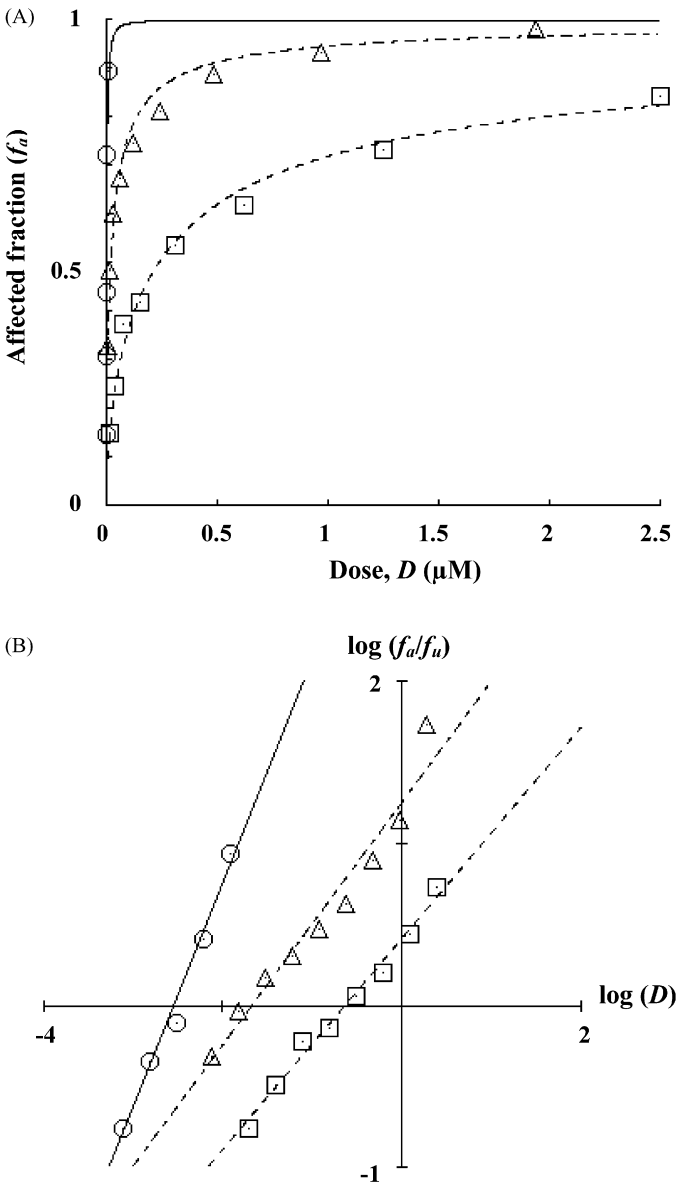

Fig. 1. (A) Dose–effect curves and (B) the median-effect plots of SOS (◯), DOX (□), and SOS + DOX combination (△) of A498 cells, according to Eqs. (1) and (2).

DRI value for each corresponding drug was calculated by the following simple equation:

$$DRI = \frac{(D_x)_1}{(D)_1} + \frac{(D_x)_2}{(D)_2} \quad (4)$$

2.8. Statistical analysis

All mean values are presented as means ± standard deviation (S.E.M.). The Student's t-test (two-tailed) was used to evaluate the statistical significance of any differences in mean values in the experimental groups. The ANOVA-test was used to assess the differences in means between single agents and combination treatments. In all statistical analyses, p-values < 0.05 were considered to indicate statistical significance.

3. Results and discussion

3.1. Characteristics of HPMA copolymer–SOS/–DOX/–Mce_6 conjugates

P-GFLG-SOS, P-GFLG-DOX and P-GFLG-Mce_6 conjugates were synthesized as shown in Scheme 1. The GFLG oligopeptide sequence was chosen as the drug attachment/release site and incorporated in all three conjugates. This tetrapeptidyl linker was designed to be stable in blood plasma, but susceptible to cleavage by cathepsin B (lysosomal cysteine proteinase) within the lysosomal compartment (Kopeček and Rejmanová, 1983; Rejmanová et al., 1983; Kopeček, 1984).

The characteristics of the conjugates, including the drug content in mol% and mol/gram of polymer conjugate, average amount of drug per macromolecule, molecular weight, and polydispersity, are summarized in Table 1. The drug content in all conjugates was similar. P-GFLG-SOS, P-GFLG-DOX and P-GFLG-Mce_6 conjugates contained 3.4, 3.0, and 2.9 drug molecules per macromolecule, respectively. The apparent M_w of polymer conjugates was estimated by size exclusion chromatography using ÄKTA system, equipped with a Superose 6 HR 10/30 column calibrated with poly(HPMA) samples. The apparent M_w of the polymer conjugates was between 23 and 32 kDa, whereas the polydispersity ranged from 1.2 to 1.5.

3.2. In vitro inhibition of A498 cell growth by drugs as single agents

Renal cell carcinoma is the predominant form of kidney cancer and highly refractory to chemotherapy due to the multidrug resistance. This is due to gp-170, a membranous glycoprotein encoded by the MDR1 gene (Vugrin, 1987). The A498 cell line is a primary renal carcinoma cell line that expresses a moderate level of gp-170 (Yu et al., 1998). Moreover, A498 cell has been reported to express a functional wild-type p53. The transcriptional activity of p53 in renal cell carcinoma is significantly regulated by MDM-2 (mouse double minute-2) (Warburton et al., 2005).

SOS has a pronounced antitumor activity toward tumor cells lines expressing wild-type p53, especially the A498 human renal carcinoma cell line. SOS molecule interrupts the p53–HDM-2 interaction (Issaeva et al., 2004), induces DNA damage and generates DNA–protein and DNA–DNA crosslinks (Nieves-Neira et al., 1999). These effects lead to p53 stabilization and activation, resulting in G_0–G_1 and G_2–M cell cycle arrest, thereby strongly inducing apoptosis. *In vivo* studies of SOS in mice with xenografts derived from different drug-sensitive cell lines, including renal A498, renal CAKI-1, melanoma UACC-257, ovarian OVCAR-5, colon HCC-2998 (Rivera et al., 1999), colon HCT116 expressing wild-type p53 and its derivative p53-null HCT116 (Issaeva et al., 2004), showed that SOS possessed strong antitumor activity. It produced complete tumor regression of A498 tumor xenografts, and possessed a moderate or minimal antitumor activity to other cell lines, but had no effect on p53-null HCT116 xenografts.

DOX is one of the most widely used chemotherapeutic agents with multiple mechanisms of action, including: intercalating DNA (Neidle, 1979), inhibiting DNA–topoisomerase II interaction (Tewey et al., 1984), and inducing the generation of singlet oxygen and other oxygen radicals (Sinha et al., 1987). These mechanisms lead to DNA strand breaks, DNA damage, and damage to cellular membranes, resulting in G_1 and G_2 cell cycle arrest and cell death (Fornari et al., 1994; Blagosklonny, 2002; Larsen et al., 2003). *In vitro* studies of DOX cytotoxicity toward renal carcinoma cell lines have shown that they are sensitive to DOX, especially the A498 cell line (Mertins et al., 2001; Yu et al., 1998). However, the usefulness of DOX is limited by side effects, particularly cumulative dose-dependent cardiotoxicity (Shan et al., 1996). Previous studies in mice have demonstrated that the severe cardiotoxicity of DOX can be reduced by conjugating it to HPMA copolymers (Seymour et al., 1990). Similar results have been observed in clinical trials (Vasey et al., 1999).

Photodynamic therapy is a three-component therapy consisting of a photosensitizer, visible light and oxygen. Mce_6, a second-generation photosensitizer, is activated by a characteristic wavelength of light to an excited singlet state, which rapidly decays to the triplet state. Both singlet and triplet state species can transfer energy to surrounding oxygen (in ground triplet state) to produce singlet oxygen. Singlet oxygen is highly reactive and will oxidize biomolecules, resulting in irreversible photodamage to the cells, cell destruction, and cell death (Hopper, 2000; Dolmans et al., 2003). Common side effects are prolonged cutaneous and systemic photosensitivities, which remain a problem in patients treated with low-molecular weight photosensitizers (Dougherty et al., 1990; Chiarello, 2004). Binding Mce_6 to HPMA copolymers containing a targeting moiety can also limit its distribution in the body and reduce side effects (Krinick et al., 1990; Goff et al., 1991; Shiah et al., 2001b).

The inhibitory effects of SOS, DOX, Mce_6, P-GFLG-SOS, P-GFLG-DOX, and P-GFLG-Mce_6 as single agents on the growth of A498 cells were evaluated after 16 h of drug exposure using the MTT assay. Values collected using untreated control cells corresponded to 100% cell viability. The IC_{50} values for the free drugs and the HPMA copolymer conjugates are shown in Table 2. The A498 cell line was highly susceptible to SOS and P-GFLG-SOS with IC_{50} values of 3 and 23 nM, respectively. The IC_{50} of SOS in this study was in agreement with that measured

Table 2
Cell proliferation IC_{50} values for SOS, DOX, Mce_6, and their HPMA copolymer conjugates against A498 cells

Drug	IC_{50} or D_m (μM)[a]
SOS	0.003 ± 0.0003[b]
DOX	0.24 ± 0.02[b]
Mce_6	3.55 ± 0.08[b]
P-GFLG-SOS	0.023 ± 0.0004[b]
P-GFLG-DOX	26.8 ± 33.4[b]
P-GFLG-Mce_6	7.32 ± 0.12[b]

[a] D_m is the median-effect dose that inhibits the cell growth by 50%. IC_{50} or D_m values are the means ± S.E.M. ($n = 6$).
[b] The differences of means against control were statistically significant at p-value < 0.05 (Student's test).

by Rivera et al., who reported an IC_{50} of 2 nM in the A498 cell line after a 48 h exposure to SOS (Rivera et al., 1999). In all experiments the linear correlation coefficient of the median-effect plot (r) was >0.98, providing a reliable basis for further calculations.

SOS was 80 and 1170 times more effective than DOX and Mce_6, respectively; P-GFLG-SOS was 1170 and 320 times more effective than P-GFLG-DOX and P-GFLG-Mce_6, respectively (Table 2). The IC_{50} values of P-GFLG-SOS, P-GFLG-DOX and P-GFLG-Mce_6 were higher than those of free SOS, DOX, and Mce_6, respectively. These results reflect the different mechanisms of cellular internalization of free drugs versus copolymer conjugates. Copolymer conjugates containing hydrophobic drugs/moieties are internalized by fluid-phase pinocytosis and adsorptive pinocytosis concurrently, which is slower than the diffusion process of free drugs (Duncan et al., 1981). The relatively low disparity between the IC_{50} doses of Mce_6 and P-GFLG-Mce_6 (3.55 μM vs. 7.32 μM) reflects the fact that it is not necessary for Mce_6 molecules to be cleaved from copolymer backbone to generate a photodynamic effect. Polymer-bound Mce_6 can also produce singlet oxygen, albeit at a lower quantum yield than free Mce_6 (Krinick et al., 1990).

The advantages of polymer-bound drugs (when compared to low-molecular weight drugs) are (reviewed in Putnam and Kopeček, 1995; Kopeček et al., 2000; Duncan, 2003): (a) active uptake by fluid-phase pinocytosis (non-targeted polymer-bound drug) or receptor-mediated endocytosis (targeted polymer-bound drug), (b) increased *active* accumulation of the drug at the tumor site using targeting (Lu et al., 1999; Shiah et al., 2001b), (c) increased *passive* accumulation of the drug at the tumor site by the enhanced permeability and retention (EPR) effect (Shiah et al., 2001a), (d) long-lasting circulation in the bloodstream (Seymour et al., 1987, 1990), (e) decreased non-specific toxicity of the conjugated drug (Říhová et al., 1988), (f) decreased immunogenicity of the targeting moiety (Říhová et al., 1988), (g) immunoprotecting and immunomobilizing activities (Říhová et al., 2001), (h) modulation of the cell signaling and apoptotic pathways (Minko et al., 1999, 2000, 2001; Nishiyama et al., 2003; Malugin et al., 2006), (i) enhanced solubility of hydrophobic drugs, and (j) the potential to overcome efflux pump-mediated mechanism of drug resistance (Minko et al., 1998, 1999, 2000).

3.3. In vitro growth inhibition of agents in combination

Experiments investigating the cytotoxicity potential of binary combinations of SOS, DOX, Mce_6, P-GFLG-SOS, P-GFLG-DOX, P-GFLG-Mce_6 against A498 cells were evaluated by exposing cells to combinations of free drugs/conjugates at ratios based on their respective IC_{50} concentrations (Table 2). Fig. 2 shows the composite dose–response curves of A498 cells indicating the anti-proliferative effects of single agents and their combinations. The dose–response curves for combined treatment were obtained by plotting cell viability (y) versus the combined dose of two single agents (x). All of the binary combination treatments showed anti-proliferative activities toward the A498 cell line. The dose ratio, IC_{50} or D_m values of the combination treatment, and dose of each drug/conjugate combination that inhibit cell growth by 50% are shown in Table 3. The dose of each drug/conjugate in combination was substantially lower than the IC_{50} doses of the drugs as single agents (compare Tables 2 and 3). These results clearly indicate that all of the combination treatments were effective against A498 cells.

To evaluate potential synergy of the combinations of free drugs and copolymer conjugates towards A498 cells *in vitro*, the combination index (CI) analysis was used (Chou and Talalay, 1984; Chou, 2006). In the CI analysis, values of CI < 1, CI = 1, and CI > 1 indicate synergy, additivity, and antagonism, respectively. Fig. 3 and Table 4 show a graphic summary of the CI analyses over all levels of effect (f_a = 0.05–0.95 or 5–95% of inhibition effect) and CI values at 25%, 50%, 75% and 95% of growth inhibition effects in A498 cells, respectively. It should be noted that at very high and at very low drug effect levels, the method is less accurate due to logarithmic transformation (Zhao et al., 2004). Consequently, we have chosen f_a from 0.05 to 0.95 for evaluation. The most synergistic binary combination was SOS + DOX. Simultaneous addition of SOS and DOX to A498 cells in a monolayer culture yielded CI values lower than 1 over the entire range of cytotoxicity, indicating a strong synergistic to moderate synergistic effect. The SOS + Mce_6 and P-GFLG-SOS + P-GFLG-Mce_6 combinations both displayed synergism

Table 3
Dose ratios and IC_{50} doses in combination treatments of free drugs (SOS + DOX, SOS + Mce_6, and DOX + Mce_6) and their copolymer conjugates (P-GFLG-SOS + P-GFLG-DOX, P-GFLG-SOS + P-GFLG-Mce_6, and P-GFLG-DOX + P-GFLG-Mce_6) in A498 cells

Drug combination		Dose ratio	D_m (μM)[a]	D (μM)[b]	
Drug A	Drug B			Drug A	Drug B
SOS	DOX	1:80	0.0213 ± 0.002	0.00027	0.021
SOS	Mce_6	1:1330	0.270 ± 0.028	0.00020	0.27
DOX	Mce_6	1:16.7	0.392 ± 0.18	0.022	0.37
P-GFLG-SOS	P-GFLG-DOX	1:1200	1.37 ± 0.052	0.0011	1.37
P-GFLG-SOS	P-GFLG-Mce_6	1:280	1.48 ± 0.291	0.0053	1.47
P-GFLG-DOX	P-GFLG-Mce_6	1:0.23	3.71 ± 0.337	3.01	0.70

[a] D_m represent the mean ± S.E.M. (n = 6). The statistical comparisons in D_m between single agent treatments (Table 2) and combination treatments (Table 3) were significant at p-value < 0.05 (ANOVA).

[b] D is the dose of each drug/conjugate in a combination that inhibits the cell growth by 50%.

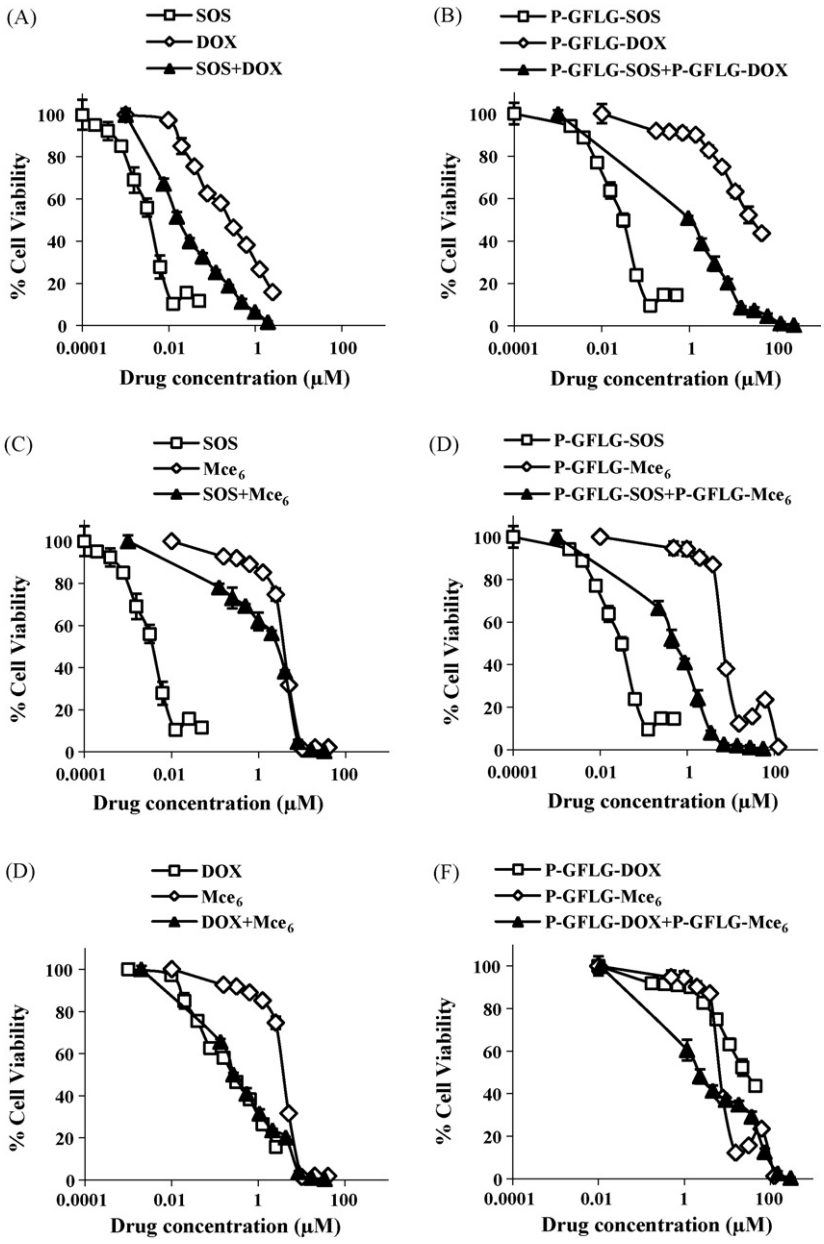

Fig. 2. Dose–response curves of A498 cells treated with (A) SOS and DOX, (B) P-GFLG-SOS and P-GFLG-DOX, (C) SOS and Mce_6, (D) P-GFLG-SOS and P-GFLG-Mce_6, (E) DOX and Mce_6, (F) P-GFLGDOX and P-GFLG-Mce_6, as single agents and binary combinations at constant ratios of their respective IC_{50} concentrations; bars represent the standard error ($n = 6$).

Table 4
Combination index values at different effect levels for combination treatments of A498 cells with free and HPMA copolymer-bound drugs

Drug combination		Combination index (CI)[a]			
Drug A	Drug B	IC_{25}	IC_{50}	IC_{75}	IC_{95}
SOS	DOX	0.16 ± 0.02	0.18 ± 0.01	0.25 ± 0.02	0.60 ± 0.17
SOS	Mce_6	0.34 ± 0.08	0.45 ± 0.08	0.64 ± 0.11	1.33 ± 0.38
DOX	Mce_6	0.23 ± 0.04	0.20 ± 0.03	0.27 ± 0.03	0.77 ± 0.16
P-GFLG-SOS	P-GFLG-DOX	0.46 ± 0.07	0.54 ± 0.06	0.66 ± 0.06	0.97 ± 0.15
P-GFLG-SOS	P-GFLG-Mce_6	0.69 ± 0.05	0.77 ± 0.05	0.88 ± 0.07	1.19 ± 0.13
P-GFLG-DOX	P-GFLG-Mce_6	0.20 ± 0.06	0.21 ± 0.04	0.31 ± 0.06	1.02 ± 0.66

[a] Combination index (CI) values <1, =1, and >1 characterize synergism, additive effect, and antagonism, respectively. CI values shown are mean ± S.E.M. ($n = 6$).

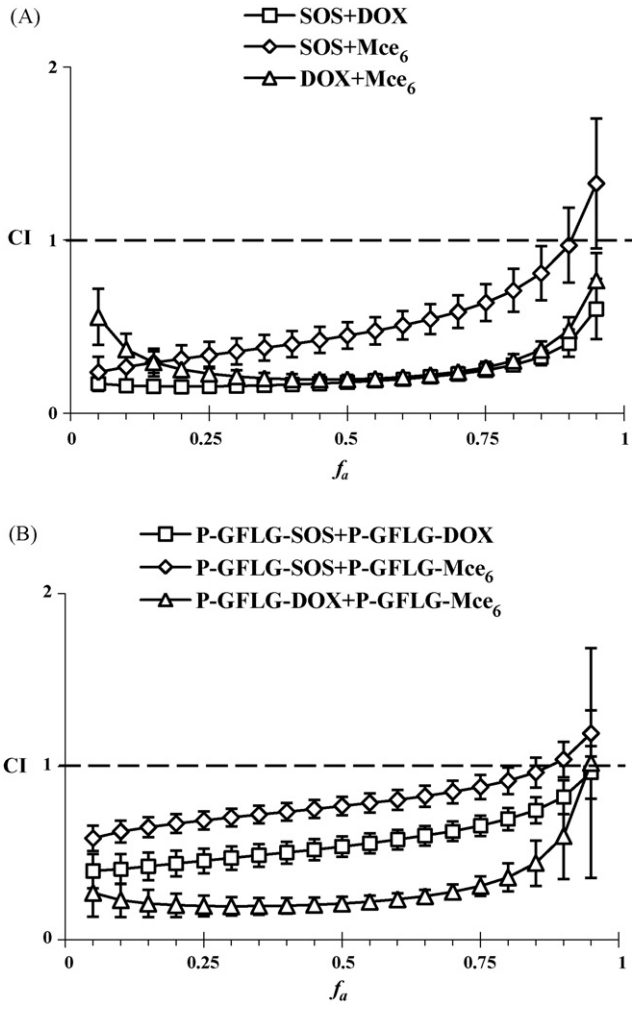

Fig. 3. Combination index plots (f_a–CI plots) obtained from median-effect analysis: (A) free drug combinations and (B) copolymer conjugate combinations. Chemotherapeutic drugs and their copolymer conjugates were graually diluted at the ratio of their IC_{50} values as a series of twofold dilutions from 8 to 0.03125 times IC_{50} and A498 cells exposed to drugs simultaneously for 16 h as described in Section 2. CI < 1, =1 and >1 indicates synergism, additive effect and antagonism, respectively. The vertical bars indicate the 95% confidence intervals based on Sequential Deletion Analysis (SDA) and can be generated by using CompuSyn software.

for f_a values up to about 0.8, but showed slight antagonism and near additivity at $f_a = 0.95$, respectively. However, all other combinations were synergistic to varying degrees up to $f_a < 0.9$, and were additive at higher f_a values. The experimental data were also analyzed using the isobologram method (Loewe, 1953). The result comparison (data not shown) indicated that both the CI and isobologram analyses produced very similar results.

The synergistic effects of combinations may depend on the cytotoxic mechanism of each agent. SOS, DOX, and Mce_6 have different sites of action, but produce similar cytotoxic intermediates and outcomes including: DNA damage, cellular damage, cell cycle arrest, and cell apoptosis. DOX + Mce_6 and P-GFLG-DOX + P-GFLG-Mce_6 combinations showed better synergistic effects compared to other combinations, probably due to the multiple mechanisms of action of DOX, including generation of reactive oxygen species (Sinha et al., 1987), which is analogous to the activity of Mce_6. The mechanism of this synergistic effect is the potentiation of PDT by DOX and vice versa. In the cell, DOX can be reduced by NADPH cytochrome P450 reductase to semiquinone-free radicals. In the presence of molecular oxygen, the semiquinone radicals are capable of enhancing superoxide production (Berlin and Haseltine, 1981; Bartoszek, 2002), which can cause damage to biological molecules. This suggests that DOX + Mce_6 and P-GFLG-DOX + P-GFLG-Mce_6 combinations produced similar cytotoxic intermediates with a concomitant enhancement of efficacy. Enhanced efficacy resulting from the combination of a photosensitizer and DOX has been demonstrated on various cell lines, such as Walker 256 carcinosarcoma cells (Edell and Cortese, 1988), H-MESO-1 human malignant mesothelioma cells (Brophy and Keller, 1992), murine L929 cells (Lanks et al., 1994), and murine hepatoma MH-22A (Kirveliene et al., 2006).

SOS + DOX and P-GFLG-SOS + P-GFLG-DOX combinations also showed synergistic effects. Both drugs act on DNA: SOS induces DNA–protein and DNA–DNA crosslinks with no detectable DNA strand breaks (Nieves-Neira et al., 1999), but DOX can intercalate into DNA strands and also produce non-protein-associated and protein-associated DNA strand breaks (Fornari et al., 1994). Regardless of the detailed mechanism, both SOS and DOX induce DNA damage, cell cycle arrest at G_1 and G_2, and, ultimately cell apoptosis.

Furthermore, many *in vivo* studies have described enhanced antitumor activity of DOX in combination with other chemotherapeutic agents. Examples include: the combination of immunoconjugate BR96-DOX and paclitaxel against MCF7 human breast carcinoma, L2987 human lung carcinoma, RCA and LS174T human colon carcinomas in athymic mice (Trail et al., 1999), doxorubicin with anti-fetal liver kinase 1 monoclonal antibody in human SKLMS-1 leiomysarcoma and RD rhabdomyosacoma xenografts in SCID mice (Zhang et al., 2002), pegylated liposomal doxorubicin administered with nanoliposomal topotecan for treatment of intracranial brain tumor xenografts (Yamashita et al., 2007), and the combination of liposomal doxorubicin and topotecan, docetaxel, gemcitabine, capecitabine, or celecoxib for treatment of OVCAR-3 and ES-2 human ovarian carcinoma xenografts (Saucier et al., 2007).

SOS + Mce_6 and P-GFLG-SOS + P-GFLG-Mce_6 combinations showed weaker synergistic effects than the other combinations. It is not clear how the facts, that SOS and Mce_6 have different mechanisms of action and produce different cytotoxic intermediates, relate to this phenomenon.

The DRI values in Table 5 indicate the fraction that the drug concentrations can be decreased to achieve the IC_{50}. For example, the IC_{50} value was 0.003 μM SOS or 0.24 μM DOX in single agent treatments (Table 2), but a 1:80 combination of SOS + DOX can inhibit 50% of cell growth using 0.00027 μM SOS and 0.021 μM DOX. This represents an 11-fold decrease for both SOS and DOX concentrations. All combinations produced IC_{50} values with DRIs ranging from 4.5 to 20.5. These results indicated that the median-effect dose of each agent could be reduced when used in combination and consequently reduce the non-specific side effect of each agent.

Table 5
Dose-reduction index values at 50% effect levels of combined treatments of free drugs and their copolymer conjugates in A498 cells

Drug combination		Dose-reduction index (DRI)[a]	
Drug A	Drug B	Drug A	Drug B
SOS	DOX	11.16 ± 1.38	11.12 ± 0.42
SOS	Mce_6	14.96 ± 0.53	13.36 ± 1.73
DOX	Mce_6	10.74 ± 1.28	9.62 ± 1.30
P-GFLG-SOS	P-GFLG-DOX	20.50 ± 0.93	19.52 ± 1.37
P-GFLG-SOS	P-GFLG-Mce_6	4.46 ± 0.05	4.97 ± 0.42
P-GFLG-DOX	P-GFLG-Mce_6	8.90 ± 0.50	10.42 ± 1.61

[a] Dose-reduction index (DRI) values at IC_{50} (or D_m) were determined using $DRI = (D_x)/(D)$ (see Section 2). DRI values represent mean ± S.E.M. ($n = 6$).

Previously, *in vitro* studies of the interaction between free DOX and Mce_6 using the isobologram method (Peterson et al., 1995) and the cooperation between free and HPMA copolymer–DOX and HPMA copolymer–Mce_6 conjugates (Lu et al., 1999) in human ovarian OVCAR-3 carcinoma cells demonstrated that the combination DOX + Mce_6 decreased the percentage of viable cells and displayed synergistic-to-additive effects in the dose range tested. P-GFLG-DOX improved the efficacy of P-GFLG-Mce_6 when the variable dose of P-GFLG-DOX was simultaneously added to an effective dose of P-GFLG-Mce_6. By contrast, P-GFLG-Mce_6 did not significantly improve the efficacy profile of P-GFLG-DOX when the variable dose of P-GFLG-Mce_6 was simultaneously added to an effective dose of P-GFLG-DOX (Lu et al., 1999).

Recently, Vicent and collaborators (Greco et al., 2005; Vicent et al., 2005) have synthesized an HPMA copolymer conjugate containing both DOX and the aromatase inhibitor aminoglutethimide (AGM) attached to one macromolecule and evaluated its biological activity toward MCF-7 and MCF-7ca breast cancer cells. Their results showed that HPMA copolymer bearing both DOX and AGM on one macromolecule showed increased cytotoxicity *in vitro*, while a combination of P-GFLG-DOX and HPMA copolymer-bound AGM (P-GFLG-AGM) exhibited low toxicity. The mechanism is unknown, but is probably related to differences in the subcellular pharmacokinetics of one conjugate versus the combination of two conjugates possessing one drug.

Recently, many researchers have focused on drug combinations *in vivo* and in clinical trials to determine the synergism or antagonism of combined drugs in order to lower dosages and reduce side effects. A recently published review of clinical studies of combination treatments of renal cell carcinoma (Amato, 2005) showed five different combination regimens with 5–71% antitumor response along with acceptable toxicity profiles. Hainsworth et al. studied the clinical efficacy and toxicity of combined treatment of metastatic renal cell carcinoma with bevacizumab and erlotinib in a phase II trial. It was demonstrated that both targeted agents in combination were effective and well tolerated (Hainsworth et al., 2005). Using drug combinations with different drug exposure schedules, or simultaneous versus consecutive exposure, may result in different antitumor activities. For example, the combination of a bis-phenazine (XR5944) with 5-fluorouracil (5-FU) and irinotecan, simultaneously or sequentially, against colon cancer HT29 cell line showed that simultaneous exposure of cells to XR5944 and 5-FU or irinotecan exhibited antagonism, while sequential exposure to either order of these drugs displayed additive effects or better (Harris et al., 2005).

4. Conclusions

Combinations of free and HPMA copolymer-bound SOS, DOX, and Mce_6 produced synergistic effects in the treatment of A498 renal carcinoma cells. This bodes well for further development of macromolecular nanomedicines based on HPMA copolymers. Several HPMA copolymer drug conjugates underwent clinical testing, including DOX (Vasey et al., 1999) and platinates (Rademaker-Lakhai et al., 2004). The advantages of combination therapy using HPMA copolymer conjugates have been demonstrated on animal models of ovarian carcinoma (Krinick et al., 1994; Peterson et al., 1996; Shiah et al., 1999, 2000, 2001b). The results presented here highlight the potential applications of synergistic combinations and dose reduction for combination therapy for renal carcinoma. These observations may prove useful in the development of *in vivo* combination study protocols for the treatment of renal cancer and could be further confirmed in future clinical applications.

Acknowledgements

The research was supported in part by the NIH grant CA51578 from the National Cancer Institute and by the Royal Golden Jubilee Ph.D. Program (PHD/0176/2545) from Thailand. We thank Jon Callahan for carefully editing the manuscript.

References

Alley, M.C., Hollingshead, M.G., Dykes, D.J., Waud, W.R., 2004. Human tumor xenograft models in NCI drug development. In: Teicher, B.A., Andrews, P.A. (Eds.), Anticancer Drug Development Guide: Preclinical Screening, Clinical Trials, and Approval. Humana Press, NJ, pp. 125–152.

Amato, R.J., 2005. Renal cell carcinoma: review of novel single-agent therapeutics and combination regimens. Ann. Oncol. 16, 7–15.

Bartoszek, A., 2002. Metabolic activation of adriamycin by NADPH-cytochrome P450 reductase; overview of its biological and biochemical effects. Acta Biochim. Pol. 49, 323–331.

Berlin, V., Haseltine, W.A., 1981. Reduction of adriamycin to a semiquinone-free radical by NADPH cytochrome P-450 reductase produces DNA cleavage in a reaction mediated by molecular oxygen. J. Biol. Chem. 256, 4747–4756.

Blagosklonny, M.V., 2002. Sequential activation and inactivation of G2 checkpoints for selective killing of p53-deficient cells by microtubule-active drugs. Oncogene 21, 6249–6254.

Brophy, P.F., Keller, S.M., 1992. Adriamycin enhanced in vitro and in vivo photodynamic therapy of mesothelioma. J. Surg. Res. 52, 631–634.

Buchegger, F., Allal, A.S., Roth, A., Papazyan, J.P., Dupertuis, Y., Mirimanoff, R.O., Gillet, M., Pelegrin, A., Mach, J.P., Slosman, D.O., 2000. Combined radioimmunotherapy and radiotherapy of liver metastases from colorectal cancer: a feasibility study. Anticancer Res. 20, 1889–1896.

Chiarello, K., 2004. In between the light and the dark. Pharm. Technol. 28, 48–54.

Chou, T.C., 1976. Derivation and properties of Michaelis–Menten type and Hill type equations for reference ligands. J. Theor. Biol. 59, 253–276.

Chou, T.C., 2006. Theoretical basis, experimental design, and computerized simulation of synergism and antagonism in drug combination studies. Pharmacol. Rev. 58, 621–681.

Chou, T.C., Martin, N., 2006. A Computer Program for Quantitation of Synergism and Antagonism in Drug Combinations and the Determination of IC_{50} and ED_{50} Values. ComboSyn Inc., New York.

Chou, T.C., Talalay, P., 1984. Quantitative analysis of dose–effect relationships: the combined effects of multiple drugs or enzyme inhibitors. Adv. Enzyme Regul. 22, 27–55.

Colasanti, A., Kisslinger, A., Quarto, M., Riccio, P., 2004. Combined effects of radiotherapy and photodynamic therapy on an in vitro human prostate model. Acta Biochim. Pol. 51, 1039–1046.

Dasmahapatra, G.P., Didolkar, P., Alley, M.C., Ghosh, S., Sausville, E.A., Roy, K.K., 2004. In vitro combination treatment with perifosine and UCN-01 demonstrates synergism against prostate (PC-3) and lung (A549) epithelial adenocarcinoma cell lines. Clin. Cancer Res. 10, 5242–5252.

Dolmans, D.E., Fukumura, D., Jain, R.K., 2003. Photodynamic therapy for cancer. Nat. Rev. Cancer 3, 380–387.

Dougherty, T.J., Cooper, M.T., Mang, T.S., 1990. Cutaneous phototoxic occurrences in patients receiving Photofrin. Lasers Surg. Med. 10, 485–488.

Duncan, R., 2003. The dawning era of polymer therapeutics. Nat. Rev. Drug Discov. 2, 347–360.

Duncan, R., Rejmanová, P., Kopeček, J., Lloyd, J.B., 1981. Pinocytic uptake and intracellular degradation of *N*-(2-hydroxypropyl) methacrylamide copolymers. A potential drug delivery system. Biochim. Biophys. Acta 678, 143–150.

Edell, E.S., Cortese, D.A., 1988. Combined effects of hematoporphyrin derivative phototherapy and adriamycin in a murine tumor model. Lasers Surg. Med. 8, 413–417.

Fischer, P.M., Lane, D.P., 2004. Small-molecule inhibitors of the p53 suppressor HDM2: have protein–protein interactions come of age as drug targets? Trends Pharmacol. Sci. 25, 343–346.

Fornari, F.A., Randolph, J.K., Yalowich, J.C., Ritke, M.K., Gewirtz, D.A., 1994. Interference by doxorubicin with DNA unwinding in MCF-7 breast tumor cells. Mol. Pharmacol. 45, 649–656.

Frei III, E., Karon, M., Levin, R.H., Freireich, E.J., Taylor, R.J., Hananian, J., Selawry, O., Holland, J.F., Hoogstraten, B., Wolman, I.J., Abir, E., Sawitsky, A., Lee, S., Mills, S.D., Burgert Jr., E.O., Spurr, C.L., Patterson, R.B., Ebaugh, F.G., James III, G.W., Moon, J.H., 1965. The effectiveness of combinations of antileukemic agents in inducing and maintaining remission in children with acute leukemia. Blood 26, 642–656.

Goff, B.A., Bamberg, M., Hasan, T., 1991. Photoimmunotherapy of human ovarian carcinoma cells ex vivo. Cancer Res. 51, 4762–4767.

Greco, F., Vicent, M.J., Penning, N.A., Nicholson, R.I., Duncan, R., 2005. HPMA copolymer–aminoglutethimide conjugates inhibit aromatase in MCF-7 cell lines. J. Drug Target. 13, 459–470.

Hainsworth, J.D., Sosman, J.A., Spigel, D.R., Edwards, D.L., Baughman, C., Greco, A., 2005. Treatment of metastatic renal cell carcinoma with a combination of bevacizumab and erlotinib. J. Clin. Oncol. 23, 7889–7896.

Hansen, M.B., Nielsen, S.E., Berg, K., 1989. Re-examination and further development of a precise and rapid dye method for measuring cell growth/cell kill. J. Immunol. Methods 119, 203–210.

Harris, S.M., Mistry, P., Freathy, C., Brown, J.L., Charlton, P.A., 2005. Antitumour activity of XR5944 in vitro and in vivo in combination with 5-fluorouracil and irinotecan in colon cancer cell lines. Br. J. Cancer 92, 722–728.

Hopper, C., 2000. Photodynamic therapy: a clinical reality in the treatment of cancer. Lancet Oncol. 1, 212–219.

Issaeva, N., Bozko, P., Enge, M., Protopopova, M., Verhoef, L.G., Masucci, M., Pramanik, A., Selivanova, G., 2004. Small molecule RITA binds to p53, blocks p53-HDM-2 interaction and activates p53 function in tumors. Nat. Med. 10, 1321–1328.

Jin, M.L., Yang, B.Q., Zhang, W., Ren, P., 1992. Combined treatment with photodynamic therapy and chemotherapy for advanced cardiac cancers. J. Photochem. Photobiol. B 12, 101–106.

Kim, W.J., Kakehi, Y., Kinoshita, H., Arao, S., Fukumoto, M., Yoshida, O., 1996. Expression patterns of multidrug-resistance (MDR1), multidrug resistance-associated protein (MRP), glutathione-*S*-transferase-pi (GST-pi) and DNA topoisomerase II (Topo II) genes in renal cell carcinomas and normal kidney. J. Urol. 156, 506–511.

Kirveliene, V., Grazeliene, G., Dabkeviciene, D., Micke, I., Kirvelis, D., Juodka, B., Didziapetriene, J., 2006. Schedule-dependent interaction between doxorubicin and mTHPC-mediated photodynamic therapy in murine hepatoma in vitro and in vivo. Cancer Chemother. Pharmacol. 57, 65–72.

Kopeček, J., 1984. Controlled biodegradability of polymers—a key to drug delivery systems. Biomaterials 5, 19–25.

Kopeček, J., Krinick, N.L., 1993. Drug delivery system for the simultaneous delivery of drugs activatable by enzymes and light. US Patent 5,258,453, November 2.

Kopeček, J., Rejmanová, P., 1983. Enzymatically degradable bonds in synthetic polymers. In: Bruck, S.D. (Ed.), Controlled Drug Delivery, vol. 1. CRC Press, FL, pp. 81–124.

Kopeček, J., Rejmanová, P., Strohalm, J., Ulbrich, K., Říhová, B., Chytrý, V., Lloyd, J., Duncan, R., 1991. Synthetic polymeric drugs. US Patent 5,037,883 (August 6).

Kopeček, J., Kopečková, P., Minko, T., Lu, Z., 2000. HPMA copolymer–anticancer drug conjugates: design, activity, and mechanism of action. Eur. J. Pharm. Biopharm. 50, 61–81.

Krinick, N.L., Říhová, B., Ulbrich, K., Strohalm, J., Kopeček, J., 1990. Targetable photoactivatable drugs. 2. Synthesis of *N*-(2-hydroxypropyl)methacrylamide copolymer anti-thy 1.2 antibody-chlorin e_6 conjugates and a preliminary study of their photodynamic effect on mouse splenocytes in vitro. Makromol. Chem. 191, 839–856.

Krinick, N.L., Sun, Y., Joyner, D., Spikes, J.D., Straight, R.C., Kopeček, J., 1994. A polymeric drug delivery system for the simultaneous delivery of drugs activatable by enzymes and/or light. J. Biomater. Sci. Polym. 5, 303–324.

Lanks, K.W., Gao, J.P., Sharma, T., 1994. Photodynamic enhancement of doxorubicin cytotoxicity. Cancer Chemother. Pharmacol. 35, 17–20.

Larsen, A.K., Escargueil, A.E., Skladanowski, A., 2003. From DNA damage to G2 arrest: the many roles of topoisomerase II. Prog. Cell Cycle Res. 5, 295–300.

Loewe, S., 1953. The problem of synergism and antagonism of combined drugs. Arzneimittelforschung 3, 285–290.

Lu, J.M., Peterson, C.M., Guo-Shiah, J., Gu, Z.W., Peterson, C.A., Straight, R.C., Kopeček, J., 1999. Cooperativity between free and *N*-(2-hydroxypropyl)methacrylamide copolymer bound adriamycin and meso-chlorin e_6 monoethylene diamine induced photodynamic therapy in human epithelial ovarian carcinoma in vitro. Int. J. Oncol. 15, 5–16.

Malugin, A., Kopečková, P., Kopeček, J., 2006. HPMA copolymer-bound doxorubicin induces apoptosis in ovarian carcinoma cells by the disruption of mitochondrial function. Mol. Pharm. 3, 351–361.

Mertins, S.D., Myers, T.G., Hollingshead, M., Dykes, D., Bodde, E., Tsai, P., Jefferis, C.A., Gupta, R., Linehan, W.M., Alley, M., Bates, S.E., 2001. Screening for and identification of novel agents directed at renal cell carcinoma. Clin. Cancer Res. 7, 620–633.

Mickisch, G., Bier, H., Bergler, W., Bak, M., Tschada, R., Alken, P., 1990. P-170 glycoprotein, glutathione and associated enzymes in relation to chemoresistance of primary human renal cell carcinomas. Urol. Int. 45, 170–176.

Minko, T., Kopečková, P., Pozharov, V., Kopeček, J., 1998. HPMA copolymer bound adriamycin overcomes MDR1 gene encoded resistance in a human ovarian carcinoma cell line. J. Control. Rel. 54, 223–233.

Minko, T., Kopečková, P., Kopeček, J., 1999. Chronic exposure to HPMA copolymer-bound adriamycin does not induce multidrug resistance in a human ovarian carcinoma cell line. J. Control. Rel. 59, 133–148.

Minko, T., Kopečková, P., Kopeček, J., 2000. Efficacy of the chemotherapeutic action of HPMA copolymer-bound doxorubicin in a solid tumor model of ovarian carcinoma. Int. J. Cancer 86, 108–117.

Minko, T., Kopečková, P., Kopeček, J., 2001. Mechanisms of anticancer action of HPMA copolymer-bound doxorubicin. Macromol. Symp. 172, 35–47.

Nahabedian, M.Y., Cohen, R.A., Contino, M.F., Terem, T.M., Wright, W.H., Berns, M.W., Wile, A.G., 1988. Combination cytotoxic chemotherapy with cisplatin or doxorubicin and photodynamic therapy in murine tumors. J. Natl. Cancer Inst. 80, 739–743.

Neidle, S., 1979. The molecular basis for the action of some DNA-binding drugs. Prog. Med. Chem. 16, 151–221.

Nieves-Neira, W., Rivera, M.I., Kohlhagen, G., Hursey, M.L., Pourquier, P., Sausville, E.A., Pommier, Y., 1999. DNA protein cross-links produced by NSC 652287, a novel thiophene derivative active against human renal cancer cells. Mol. Pharmacol. 56, 478–484.

Nishiyama, N., Nori, A., Malugin, A., Kasuya, Y., Kopečková, P., Kopeček, J., 2003. Free and *N*-(2-hydroxypropyl)methacrylamide copolymer-bound geldanamycin derivative induce different stress responses in A2780 human ovarian carcinoma cells. Cancer Res. 63, 7876–7882.

Peterson, C.M., Lu, J.M., Gu, Z.W., Shiah, J.G., Lythgoe, K., Peterson, C.A., Straight, R.C., Kopeček, J., 1995. Isobolographic assessment of the interaction between adriamycin and photodynamic therapy with meso-chlorin e_6 monoethylene diamine in human epithelial ovarian carcinoma (OVCAR-3) in vitro. J. Soc. Gynecol. Invest. 2, 772–777.

Peterson, C.M., Lu, J.M., Sun, Y., Peterson, C.A., Shiah, J.G., Straight, R.C., Kopeček, J., 1996. Combination chemotherapy and photodynamic therapy with *N*-(2-hydroxypropyl)methacrylamide copolymer-bound anticancer drugs inhibit human ovarian carcinoma heterotransplanted in nude mice. Cancer Res. 56, 3980–3985.

Poindessous, V., Koeppel, F., Raymond, E., Cvitkovic, E., Waters, S.J., Larsen, A.K., 2003. Enhanced antitumor activity of irofulven in combination with 5-fluorouracil and cisplatin in human colon and ovarian carcinoma cells. Int. J. Oncol. 23, 1347–1355.

Putnam, D., Kopeček, J., 1995. Polymer conjugates with anticancer activity. Adv. Polym. Sci. 122, 55–123.

Rademaker-Lakhai, J.M., Terret, C., Howell, S.B., Baud, C.M., De Boer, R.F., Pluim, D., Beijnen, J.H., Schellens, J.H., Droz, J.P., 2004. A phase I and pharmacological study of the platinum polymer AP5280 given as an intravenous infusion once every 3 weeks in patients with solid tumors. Clin. Cancer Res. 10, 3386–3395.

Rejmanová, P., Pohl, J., Baudyš, M., Kostka, V., Kopeček, J., 1983. Polymers containing enzymatically degradable bonds. 8. Degradation of oligopeptide sequences in *N*-(2-hydroxypropyl)methacrylamide copolymers by bovine spleen cathepsin B. Makromol. Chem. 184, 2009–2020.

Říhová, B., Kopečková, P., Strohalm, J., Rossmann, P., Větvička, V., Kopeček, J., 1988. Antibody-directed affinity therapy applied to the immune system: in vivo effectiveness and limited toxicity of daunomycin conjugated to HPMA copolymers and targeting antibody. Clin. Immunol. Immunopathol. 46, 100–114.

Říhová, B., Strohalm, J., Hoste, K., Jelínková, M., Hovorka, O., Kovář, M., Plocová, D., Šírová, M., Št'astný, M., Schacht, E., Ulbrich, K., 2001. Immunoprotective therapy with targeted anticancer drugs. Macromol. Symp. 172, 21–28.

Rivera, M.I., Stinson, S.F., Vistica, D.T., Jorden, J.L., Kenney, S., Sausville, E.A., 1999. Selective toxicity of the tricyclic thiophene NSC 652287 in renal carcinoma cell lines: differential accumulation and metabolism. Biochem. Pharmacol. 57, 1283–1295.

Sachdeva, K., 2006. Renal cell carcinoma. http://www.emedicine.com/med/topic2002.htm#sectiontreatment.

Saucier, J.M., Yu, J., Gaikwad, A., Coleman, R.L., Wolf, J.K., Smith, J.A., 2007. Determination of the optimal combination chemotherapy regimen for treatment of platinum-resistant ovarian cancer in nude mouse model. J. Oncol. Pharm. Pract. 13, 39–45.

Seymour, L.W., Duncan, R., Strohalm, J., Kopeček, J., 1987. Effect of molecular weight (Mw) of *N*-(2-hydroxypropyl)methacrylamide copolymers on body distribution and rate of excretion after subcutaneous, intraperitoneal, and intravenous administration to rats. J. Biomed. Mater. Res. 21, 1341–1358.

Seymour, L.W., Ulbrich, K., Strohalm, J., Kopeček, J., Duncan, R., 1990. The pharmacokinetics of polymer-bound adriamycin. Biochem. Pharmacol. 39, 1125–1131.

Shan, K., Lincoff, A.M., Young, J.B., 1996. Anthracycline-induced cardiotoxicity. Ann. Intern. Med. 125, 47–58.

Shanks, R.H., Rizzieri, D.A., Flowers, J.L., Colvin, O.M., Adams, D.J., 2005. Preclinical evaluation of gemcitabine combination regimens for application in acute myeloid leukemia. Clin. Cancer Res. 11, 4225–4233.

Shiah, J.G., Sun, Y., Peterson, C.M., Kopeček, J., 1999. Biodistribution of free and *N*-(2-hydroxypropyl)methacrylamide copolymer-bound mesochlorin e_6 and adriamycin in nude mice bearing human ovarian carcinoma OVCAR-3 xenografts. J. Control. Rel. 61, 145–157.

Shiah, J.G., Sun, Y., Peterson, C.M., Straight, R.C., Kopeček, J., 2000. Antitumor activity of *N*-(2-hydroxypropyl)methacrylamide copolymer-mesochlorin e_6 and adriamycin conjugates in combination treatments. Clin. Cancer Res. 6, 1008–1015.

Shiah, J.G., Dvořák, M., Kopečková, P., Sun, Y., Peterson, C.M., Kopeček, J., 2001a. Biodistribution and antitumour efficacy of long-circulating *N*-(2-hydroxypropyl)methacrylamide copolymer–doxorubicin conjugates in nude mice. Eur. J. Cancer 37, 131–139.

Shiah, J.G., Sun, Y., Kopečková, P., Peterson, C.M., Straight, R.C., Kopeček, J., 2001b. Combination chemotherapy and photodynamic therapy of targetable *N*-(2-hydroxypropyl)methacrylamide copolymer–doxorubicin/mesochlorin e_6-OV-TL 16 antibody immunoconjugates. J. Control. Rel. 74, 249–253.

Sinha, B.K., Katki, A.G., Batist, G., Cowan, K.H., Myers, C.E., 1987. Differential formation of hydroxyl radicals by adriamycin in sensitive and resistant MCF-7 human breast tumor cells: implications for the mechanism of action. Biochemistry 26, 3776–3781.

Tewey, K.M., Rowe, T.C., Yang, L., Halligan, B.D., Liu, L.F., 1984. Adriamycin-induced DNA damage mediated by mammalian DNA topoisomerase II. Science 226, 466–468.

Topaly, J., Fruehauf, S., Ho, A.D., Zeller, W.J., 2002. Rationale for combination therapy of chronic myelogenous leukaemia with imatinib and irradiation or alkylating agents: implications for pretransplant conditioning. Br. J. Cancer 86, 1487–1493.

Trail, P.A., Willner, D., Bianchi, A.B., Henderson, A.J., TrailSmith, M.D., Girit, E., Lasch, S., Hellström, I., Hellström, K.E., 1999. Enhanced antitumor activity of paclitaxel in combination with the anticarcinoma immunoconjugate BR96-doxorubicin. Clin. Cancer Res. 5, 3632–3638.

Ulbrich, K., Šubr, V., Strohalm, J., Plocová, D., Jelínková, M., Říhová, B., 2000. Polymeric drugs based on conjugates of synthetic and natural macromolecules. I. Synthesis and physico-chemical characterization. J. Control. Rel. 64, 63–79.

Vasey, P.A., Kaye, S.B., Morrison, R., Twelves, C., Wilson, P., Duncan, R., Thomson, A.H., Murray, L.S., Hilditch, T.E., Murray, T., Burtles, S., Fraier, D., Frigerio, E., Cassidy, J., 1999. Phase I clinical and pharmacokinetic study of PK1 [*N*-(2-hydroxypropyl)methacrylamide copolymer doxorubicin]: first member of a new class of chemotherapeutic agents–drug–polymer conjugates. Cancer Research Campaign Phase I/II Committee. Clin. Cancer Res. 5, 83–94.

Vicent, M.J., Greco, F., Nicholson, R.I., Paul, A., Griffiths, P.C., Duncan, R., 2005. Polymer therapeutics designed for a combination therapy of hormone-dependent cancer. Angew. Chem. Int. Ed. Engl. 44, 4061–4066.

Vugrin, D., 1987. Systemic therapy of metastatic renal cell carcinoma. Semin. Nephrol. 7, 152–162.

Warburton, H.E., Brady, M., Vlatkovic, N., Linehan, W.M., Parsons, K., Boyd, M.T., 2005. p53 regulation and function in renal cell carcinoma. Cancer Res. 65, 6498–6503.

Welt, S., Ritter, G., Williams Jr., C., Cohen, L.S., Jungbluth, A., Richards, E.A., Old, L.J., Kemeny, N.E., 2003. Preliminary report of a phase I study of combination chemotherapy and humanized A33 antibody immunotherapy in patients with advanced colorectal cancer. Clin. Cancer Res. 9, 1347–1353.

Yamashita, Y., Krauze, M.T., Kawaguchi, T., Noble, C.O., Drummond, D.C., Park, J.W., Bankiewicz, K.S., 2007. Convection-enhanced delivery of a topoisomerase I inhibitor (nanoliposomal topotecan) and a topoisomerase II inhibitor (pegylated liposomal doxorubicin) in intracranial brain tumor xenografts. Neuro-Oncol. 9, 20–28.

Yu, D.S., Chang, S.Y., Ma, C.P., 1998. The expression of mdr-1-related gp-170 and its correlation with anthracycline resistance in renal cell carcinoma cell lines and multidrug-resistant sublines. Br. J. Urol. 82, 544–547.

Zhang, L., Yu, D., Hicklin, D.J., Hannay, J.A., Ellis, L.M., Pollock, R.E., 2002. Combined anti-fetal liver kinase 1 monoclonal antibody and continuous low-dose doxorubicin inhibits angiogenesis and growth of human soft tissue sarcoma xenografts by induction of endothelial cell apoptosis. Cancer Res. 62, 2034–2042.

Zhao, L., Wientjes, M.G., Au, J.L., 2004. Evaluation of combination chemotherapy: integration of nonlinear regression, curve shift, isobologram, and combination index analyses. Clin. Cancer Res. 10, 7994–8004.